Eur Phys J C **33**, s01, s956–s958 (2004)
Digital Object Identifier (DOI) 10.1140/epjcd/s2004-03-1634-2

EPJ C direct
electronic only

NESTOR first results

Apostolos G. Tsirigotis

Hellenic Open University for the NESTOR Collaboration

Received: 5 January 2004 / Accepted: 22 January 2004 /
Published Online: 3 February 2004 –

Abstract. The first floor of the NESTOR underwater neutrino telescope was successfully deployed during March 2003, fully equipped with electronics. We briefly outline the NESTOR project, the analysis methods and techniques, and we present results using 30% of the accumulated triggers.

1 Introduction

The NESTOR (Neutrino Extended Submarine Telescope with Oceanographic Research) neutrino telescope is detecting the Cerenkov radiation produced by $\nu - induced$ muons and/or showers of charged particles in a large volume of sea water. The NESTOR site is located at the South West of Peloponnese (Greece), at the seabed of the Ionian Sea. In fact this is where one finds the deepest waters in Mediterranean sea, 5200m. The NESTOR collaboration has located a $8km \times 9km$ horizontal plateau at a depth of 4000 m [1,2]. The plateau is at a mere distance of 7.5 nautical miles from shore. Extensive studies of environmental properties have been made [3,4]. These measurements show that the water transmission length is 55m at a wavelength $\lambda = 460nm$. The underwater currents have been measured and they have been found minimal, i.e. a few centimeters per second [5]. Also the sedimentology analysis is completed [6].

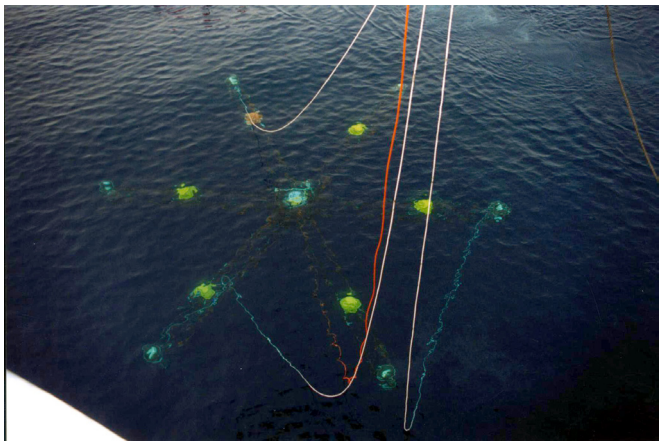

Fig. 1. A photograph of the NESTOR Floor taken during last deployment, a few moments before it was lowered to 4000m

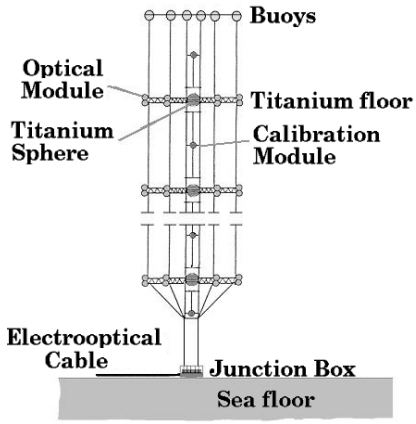

Fig. 2. NESTOR Tower

2 NESTOR detector

The basic detector unit is a rigid hexagon, shown in Fig. 1, made out of titanium with a diagonal of 32 m. At the tip of each arm of the hexagonal floor there is a pair of two 15 inch photomultiplier tubes (PMTs) inside benthos glass housings [7], one looking upwards and the other downwards. The electronics which are responsible for signal sensing, triggering, digitization and data transmission to the shore are housed inside a large titanium sphere (1m in diameter) located at the center of the hexagonal floor. The electrical pulses of the PMTs are digitized by the Analog Transient Waveform Digitizers (ATWDs) of the floor electronics board (developed at Lawrence Berkeley National Laboratory). The digitized waveforms are transmitted to shore, where the raw data are recorded. By stacking 12 of these floors in the vertical, with a distance between them 30m, they create a tower shown in Fig. 2, which is connected to the shore by an electrooptical cable (18 fibers plus 1 conductor). The effective area of a NESTOR Tower in reconstructing throughgoing muons of energy $> 10TeV$ is greater than $20000m^2$, whilst the energy threshold of such a detector is as low as 4 GeV for contained tracks.

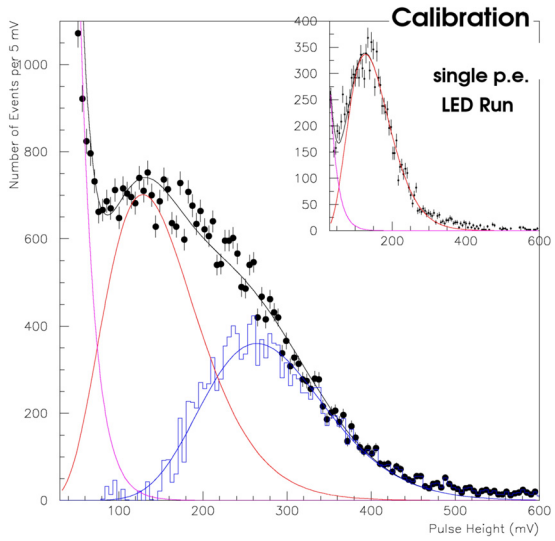

Fig. 3. The Pulse Height distribution of one PMT using data from deep sea (*main plot*) and from calibration runs (*insert plot*). The three different components correspond to the PMT dark current (*purple line*), the single photoelectron (*red line*), and the double photoelectron (*blue line*) spectrum

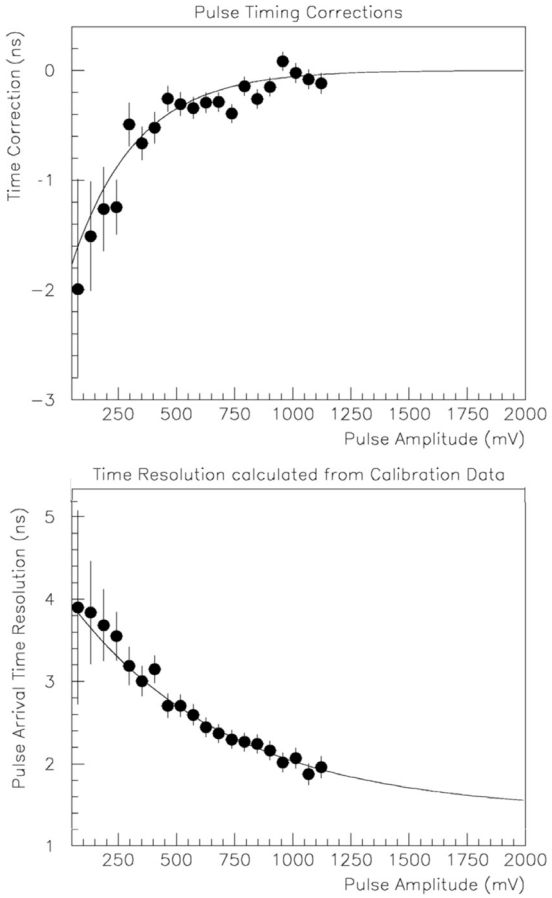

Fig. 4. Slewing correction (*top figure*) and TTS (*bottom figure*) as a function of the pulse amplitude, estimated using calibration data taken during detector operation at 4000m. They are found to agree very well with the measured ones from calibration runs in the LAB

3 Deployment

After a succesfull operation by using the cable ship TENEO of TYCOM in January 2002, an electrooptical junction box, the sea-bottom station (pyramid) with a number of associated instruments such as underwater current meter, Ocean Bottom Seismometer, nephelometers, compass, pressure gauges etc., were deployed at 4000m and connected to the end of the electrooptical cable. For the first time ever data were transmitted routinely from the deep sea in real time. Unfortunately the onset of bad weather did not allow the deployment of any other part of the detector. The NESTOR deployment techniques and methods were published in the cover article in the July issue of Sea Technology, a leading marine industry journal [8].

In March 2003, using the cable ship RAYMOND CROZE of France Telecom, the hexagonal floor shown in Fig. 1 was deployed fully equipped with electronics and associated environmental sensors to a depth of 4000m. In the control room, during the deployment and operation of the detector, the parameters of the detector were continuously monitored. These include the floor orientation (compass and tilt meters), temperatures, humidity and hygrometry within the Titanium sphere, PMT high voltages, as well as data from other environmental instruments mounted on the sea-bottom station (pyramid), such as pressure meters, current meters, etc.

4 Detector performance

The optical background due to K^{40} beta decay plus the thermionic noise from the PMTs contributes a baseline signal level of 50 kHz per PMT. This rate is constant as a function of the time and does not depend on the trigger criteria (coincidence level), demonstrating the unbias of the selection triggers. The K^{40} optical background, mainly at the single photoelectron level, can be used for calibration purposes. In Fig. 3 is shown a typical pulse height distribution of a PMT during data taking. This distribution is very well described as the overlap of the thermionic background shape and the Polya distributions for one and two photoelectrons, which have been established during the calibration runs in the laboratory.

However there are period of times where the PMT rates are significantly higher. This effect is a result of the bioluminescence activity of living organism populations. The signal bursts due to the bioluminescence activity have a variable duration 1 to 10 seconds and are easily identified and rejected. The contribution of bio-activity to the dead time of the detector has been estimated from the accumulated data to be of the order of 1% of the active experimental time.

Calibration in the sea uses LED flasher modules mounted above and below the detector floor. Using light pulses from the calibration system several experimental parameters (e.g. PMT timing, gains etc.) can be moni-

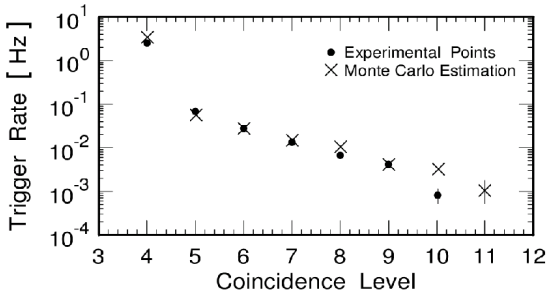

Fig. 5. Measured and Monte Carlo estimated trigger rates of $\geq$ 4-fold coincidences at the 0.25 p.e. threshold level

tored. Further analysis of the calibration data, results to in situ measurement of PMT characteristics, such as slewing Transit Time Spread (TTS). Figure 4 shows the variation at the PMT pulse arrival time and the TTS as functions of the PMT pulse amplitude, as they have been estimated from the calibration runs.

In Fig. 5 the measured trigger rates for different coincidence trigger levels are compared with the corresponding Monte Carlo estimations based on the Okada atmospheric muon flux parametrization [9], the natural K^{40} radioactivity in the sea water and PMT dark current.

In the offline analysis, the digitized waveform of each PMT has to go through a processing procedure in order to subtract baselines and to be corrected for attenuations, slewing, etc. This processing stage utilizes calibration parameters determined in the laboratory before the deployment. As a result of the signal proccessing the fast rise time of the PMT pulses is recovered (8 nsec at the single photoelectron level), multiple pulses are easily disentangled and also the arrival time, the pulse height and the total charge are accurately determined.

In order to reconstruct tracks, events with more then five active PMTs within the trigger window are selected. The estimation of the track parameters is based on χ^2 minimization using the arrival times of the PMT pulses. In most cases the procedure converges to two or occasionally several minima, often due to an inherent geometrical degeneracy. To resolve this ambiguity, a second level algorithm is used that takes account of the measured number of photoelectrons at each PMT and the number expected from the candidate track, and performs a likelihood hypothesis comparison.

Several tests of the track reconstruction procedures have been carried out using both data and Monte Carlo generated events. The results demonstrate that the estimation of the track parameters is unbiased. Figure 6 shows the measured zenith angular distribution (solid points) of reconstructed events using a fraction ($\sim 30\%$) of the collected data. The reconstructed tracks used in this measurement have been selected by means of the minimum χ^2 fit (χ^2 probability > 0.1), the track quality based on the number of photoelectrons per PMT and on the total accumulated photoelectrons per hit per track (> 4.5). The histogram shows the predicted angular distribution of atmospheric muon tracks (for the NESTOR floor geometry and reconstruction efficiency) derived from Monte Carlo calculations using Okada's phenomenological model [9].

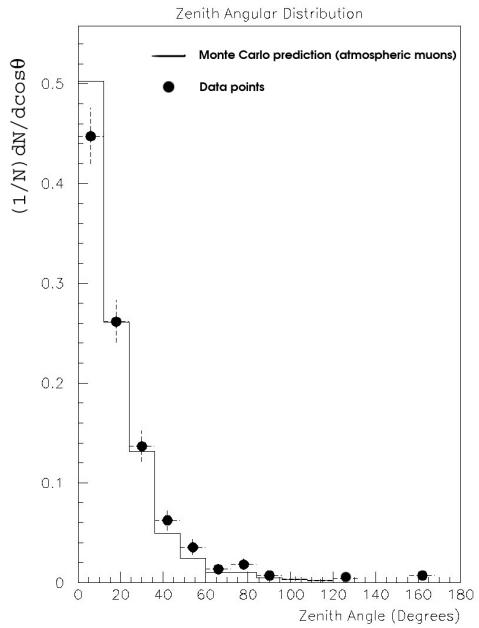

Fig. 6. Monte Carlo expectation of the zenith angular distribution of atmospheric muons at 4000m (*solid line*), compared to the zenith angular distribution of reconstructed events (*solid points*)

5 Conclusion

The NESTOR underwater neutrino telescope construction is well under way. The detector deployed is well understood and the data quality is excellent. Efficient neutrino detection will require the deployment of at least four floors, which is planned for next year.

References

1. L.K. Resvanis: (1992), 2nd NESTOR International Workshop, 1992, L. K. Resvanis editor
2. L.K. Resvanis et al.: High Energy Neutrino Astrophysics (1992), V.J. Stenger, J.G. Learned, S. Pakvasa, and X. Tata editor
3. Khanaev: (1992), 2nd NESTOR International Workshop, 1992, L.K .Resvanis editor
4. E. Anassontzis: (1994), Nuclear Instruments and Methods A **349**, 242 (1994)
5. Demidova: 2nd NESTOR International Workshop (1992), L.K. Resvanis, editor
6. E. Trimonis: 2nd NESTOR International Workshop (1992), L.K. Resvanis, editor
7. E.G. Anassontzis et.al.: "The Optical Module for the NESTOR Neutrino Telescope", NIM A **479**, 439-455 (2002)
8. E.G. Anassontzis and P. Koske: (2003), Sea Technology **44**, 10
9. A. Okada: (1994), Astroparticle Physics **2**, 393